UNDERDENSE PLASMA LENSES FOR FOCUSING PARTICLE BEAMS

T. Katsouleas, J. J. Su, and J. M. Dawson
University of California at Los Angeles
Department of Physics
Los Angeles, CA 90024 USA

Abstract

Plasma lenses are of interest for providing ultra-strong focusing of particle beams in order to enhance the luminosity of a high-energy linear collider. Previous work has explored the self-pinch of e^+ or e^- beams as they pass through an overdense slab of passive plasma (i.e., plasma density much greater than the beam density). Here we examine the focusing of beams in an underdense plasma through physical and particle simulation models. In this regime the plasma dynamics becomes highly non-linear and differs for e^+ and e^- beams. For e^- beams the plasma electrons are almost completely expelled by the beam's space charge leaving a uniform column of ion charge that provides the focusing force. Compared to the overdense lens, the underdense lens has the advantages that spherical aberrations, longitudinal aberrations, and plasma contribution to background in the detectors are all greatly reduced.

Introduction

Previous work on self-pinch plasma lenses has been mainly devoted to analytic models in the overdense plasma regime (plasma density n_o much greater than beam density n_b).[1-6] In the overdense plasma lens the beam density represented a small perturbation to the plasma density; thus, the plasma dynamics were well described by linear theory and were similar for electron and positron beams. In the underdense lens regime ($n_b \gtrsim n_o/2$), the plasma dynamics become highly non-linear and differ considerably for electrons and positrons. To describe the plasma lens in this regime we rely on physical models and self-consistent simulations. The underdense lens has several advantages including smaller spherical and longitudinal aberrations and reduced plasma contribution to background in the detectors of a collider.[7] A self-consistent example of the luminosity obtainable from e^+e^- beams focused by underdense plasma lenses shows that such lenses could enable the current SLC beams to surpass their design goal.

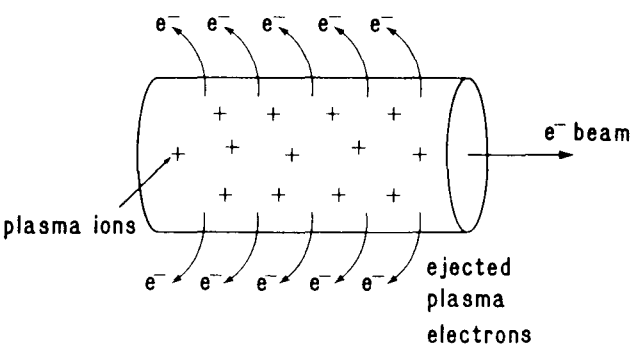

Fig. 1. Illustration of underdense plasma lens.

Physical Description

The physical mechanism of the underdense plasma lens is illustrated in Fig. 1 for e^- beams. The space charge of the e^- beam essentially blows out all of the plasma electrons leaving a uniform column of positive ion charge. The net focusing force on the e^- beam is that due to the ions' space charge since the beam's space charge and magnetic forces nearly cancel. From Gauss' law this is

$$F_r = 2\pi n_o e^2 r \ . \qquad (1)$$

When comparing Eq. (1) to the overdense lens we see that the plasma density now replaces the beam density (n_b) in determining the focusing force. Since the plasma density n_o is independent of r, the linearity of the focusing force no longer depends on the detailed radial dependence of n_b (as long as n_b is large enough to expel the plasma electrons). Thus we expect spherical aberrations to be very small for e^- beams in an underdense plasma lens.

For positron beams, the plasma dynamics are more complex. The space charge of the beam pulls plasma electrons into the beam. However, there are not enough plasma electrons available to completely neutralize the beam. Thus the plasma electron density tends to approach the positron density in the center, and to form an electron depletion region in the outer part of the beam. The focusing force becomes extremely nonlinear in r (approximately 1/r in the outer regions) in this case. A solution to this problem is then to make the beam radius small ($< (n_o/n_b)^{1/2}\, c/\omega_p$) so that the beam only samples the center region where the electron density is large and uniform. To quantitatively assess the aberrations in the underdense plasma lens we turn now to particle simulations.

Simulations

Figures 2-4 illustrate results of 2-D PIC simulations of the underdense plasma lens using the relativistic electromagnetic code ISIS[8] with coordinates $r, \theta, \rho_r, \rho_\theta, \rho_z$. From Fig. 2 for electron beams we observe first that the longitudinal aberrations inherent to the overdense lens are absent except near the front and back edges where the beam density drops below $n_o/2$. Secondly, the spherical aberrations are small enough that the beam radius has been demagnified by a factor of thirty (this implies spherical aberrations $\Delta K/K \lesssim 3\%$).

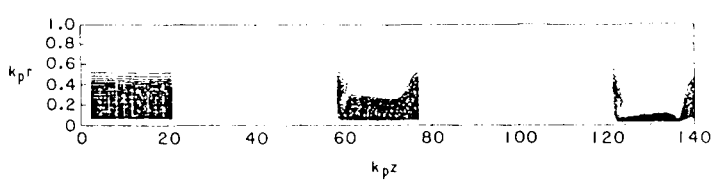

Fig. 2. Real space of e^- beam in underdense plasma lens simulation. Lens extended over $k_p z = 5$ to 25; $n_b/n_o = 2(1 - 4k_p^2 r^2)(1 - k_p^2 \xi^2/90)$; $\gamma = 1000$.

Figure 3 corresponds to Fig. 2 for a positron beam. Here the spherical aberrations are larger than in the electron case but smaller than that of the overdense lens. From the figure the density has increased by approximately 15 to 60 (suggesting $\Delta K/K \lesssim 15-25\%$). We note that for the positron case some plasma electrons were dragged out of the plasma by the space charge of the positron beam. Typically these electrons reach a few MeV and can become as dense as the positron beam. During a collision these electrons are blown out rapidly by the fields of the opposing electron beam.

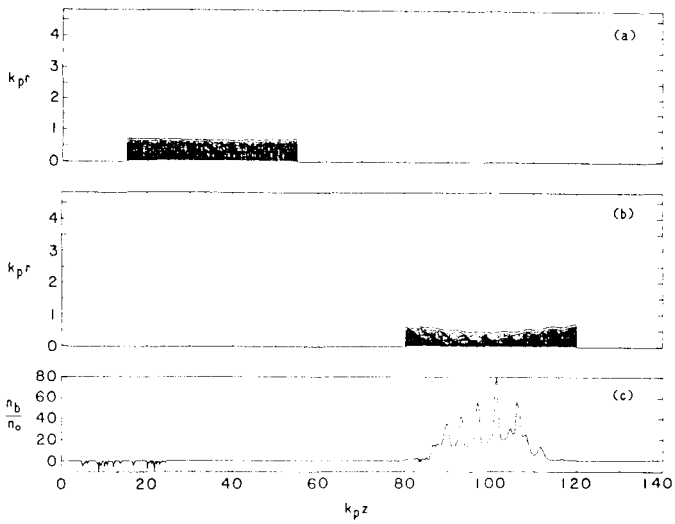

Fig. 3. Real space (a,b) and final density (c) of e^+ beam in the underdense plasma lens of Fig. 2. $n_b/n_o = 1.4\exp(-k_p^2 r^2/2\sigma_r^2 - k_p^2\xi^2/2\sigma_z^2)$, for $r < 3\sigma_r$, $|\xi| < 2\sigma_z$; $\sigma_r = .3$, $\sigma_z = 10$.

Secondly, for Gaussian radial profiles the luminosity integral over the charge densities is increased by a factor

$$L/L_o \simeq 2/(1+r^2/r_o^2) \qquad (2)$$

where r is the smaller beam radius and r_o is the larger beam radius.

Figure 4 shows the collision of the asymmetric beams after being focused by underdense lenses. Qualitatively, we see the focusing of one beam by the magnetic field of the other. It appears that tighter focusing of only one beam (i.e., the electrons) can increase the luminosity. This is for two reasons. First the denser electron beam may cause greater disruption of the positron beam.

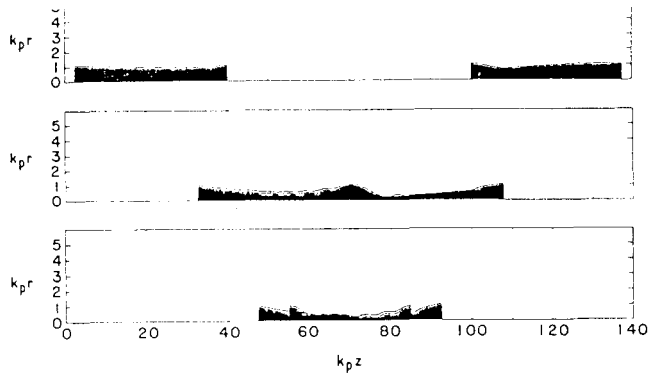

Fig. 4. Real space of colliding e^- (right) and e^+ beams showing focusing by plasma lenses and beam-beam focusing. The plasma lenses' are as in Fig. 2, centered at $k_p z = 20$ and 120; $n_b/n_p = 2(1-k_p^2 r^2)(1-k_p^2\xi^2/90)$ and $\gamma = 500$.

Discussion and SLC Example

We illustrate the conclusions of our physical and simulation models with a design example for the SLC. The SLC design goal parameters are given in the first part of Table 1. In order to meet or exceed the final spot size and luminosity goals with the plasma lens we must satisfy the following conditions: (1) The initial spot size must be small enough to avoid spherical aberration limits. From the underdense lens simulations we expect these to be of order 3% for electrons and 20% for positrons, so we must choose $\sigma_o < \sigma^*/.2 \approx 8\,\mu$. We take $\sigma_o \approx 6\mu$ (which is similar to what has been achieved to date). (2) The beam should be long and narrow compared to c/ω_p; this specifies a range of plasma densities from 10^{14} cm^{-3} to 7×10^{17} cm^{-3}. (3) The plasma density should be less than $2n_b$ to take advantage of the smaller aberrations of the underdense regime, but large enough to give strong focusing (Eq. 1). We take $n_o = 10^{17}$ cm^{-3} $\approx .8\,n_b$. (4) The thickness of the lens must be chosen large enough to overcome the emittance of the beam[10] ($\ell \gtrsim 5\times10^{11}\,\varepsilon_N/\sigma^*\sigma_o n_o$, where ε_N is the normalized emittance in cm-rads, σ^* and σ_o are in cm, and n_o is in cm^{-3}) and small enough to justify our use of a thin lens approximation. These lead us to take $\ell \approx 5.6$ mm giving f = 1 cm.

This self-consistent set of initial beam, plasma lens, and final beam parameters is summarized in Table 1. For electron beams, this plasma lens design is capable of focusing a 6μ beam to 0.5μ, enhancing the luminosity to four times the design goal (approximately two orders of magnitude higher than the initial beam luminosity entering the lens). For positron beams spherical aberrations limit the final spot size to about 20% of the initial spot size or about 1.2μ (still below the 1.6μ design goal). This suggests a luminosity of order 5×10^{30} cm^2 s^{-1} for the positron beam (without disruption). Thus the luminosity for the asymmetric collision of the two beams would be (Eq. 1) of order $5\times10^{30}\times2/(1+.5^2/1.2^2) = 8\times10^{30}$ cm^{-2} s^{-1} (without disruption). The disruption of asymmetric beams has not been treated, so we have not included this enhancement of the luminosity. Even without disruption the enhancement from the plasma lenses gives a luminosity in excess of the design goal.

Table 1. Plasma Lens Design Example

Beam Parameters

energy	50 GeV
number of particles (N)	7×10^{10}
rep. rate (ν)	180 Hz
emittance (ε)	3×10^{-8} cm–rad
bunch length (σ_z)	1 mm
initial radius (σ_o)	6 μ (design goal = 1.6 μ)

Plasma Parameters

density (n_o)	10^{17} cm^{-3} ($\simeq .8n_b$)
thickness (ℓ)	5.6 mm

Calculated Parameters

focal length (f)	1 cm	
β^*	.8 mm ($\sigma_z/\beta^* = 1.25$)	
	e^-	e^+
σ^*	.5μ	1.2μ
η (σ_z/β^*-reduction factor) from ref. 9	.7	1
$L_o\left(\frac{\eta_z \nu N^2}{4\pi\sigma^{*2}}\right)$	2.0×10^{31} cm^{-2} s^{-1}	4.8×10^{30} cm^{-2} s^{-1}
$D\left(=\frac{r_e\sigma_z N}{\gamma\sigma^{*2}}\right)$	7.8	1.4
L	3×10^{31} cm^{-2} s^{-1}	5×10^{30} cm^{-2} s^{-1}
$L_{e^+e^-}$	8×10^{30} cm^{-2} s^{-1}	

Acknowledgment

This work is support by U.S. DOE contract DE-AS03-83-ER40120, U.S. DOE grant DE-FG03-87ER13752, ONR contract no. N00014-86-K-0585 and NSF PHY 86-11235.

References

1. P. Chen, Particle Accelerators 20, 171 (1987).

2. P. Chen, J. J. Su, T. Katsouleas, S. Wilks and J. M. Dawson, IEEE Trans. Nucl. Sci. PS-15, 218 (1987).

3. J. B. Rosenzweig, B. Cole, D. J. Larson, D. B. Cline, WISC-EX-85-0000, submitted to Particle Accelerators (1987).

4. D. B. Cline, B. Cole, J. B. Rosenzweig, J. Norem, Proc. IEEE Particle Accelerator Conference, 241 (1987).

5. J. B. Rosenzweig and P. Chen, SLAC-PUB-4571, March 1988.

6. P. J. Channel in Laser Acceleration of Particles (Malibu, 1985) AIP Conference Proceedings No. 130, C. Joshi and T. Katsouleas, eds. (AIP, NY, 1985); J. D. Lawson et al., Rutherford-Appleton Laboratory Report No. RL 83057, 1983 (unpublished).

7. The effect of scattering in the plasma on beam focusing was shown to be negligible by R. G. Evans, Proc. ECFA Workshop on New Developments in Part. Accel. Techniques (Orsay, France, 1987); however, the concern here is over event noise reaching the detectors.

8. G. Gisler, M. Jones, C. Snell, Proc. 11th Int'l Conf. Num. Sim. of Plasma, (Quebec, Canada, 1985), paper 1-B-01.

9. R. Erickson, SLAC-PUB-4479, 1987.

10. J. J. Su, T. Katsouleas, J. M Dawson, R. Fedele, UCLA PPG-1177, August 1988 (submitted to Phys. Rev. A)